

# UCLA

## UCLA Previously Published Works

### Title

Single-cell RNA-seq analysis revealed long-lasting adverse effects of tamoxifen on neurogenesis in prenatal and adult brains

### Permalink

<https://escholarship.org/uc/item/66q3m76q>

### Journal

Proceedings of the National Academy of Sciences of the United States of America, 117(32)

### ISSN

0027-8424

### Authors

Lee, Chia-Ming  
Zhou, Liqiang  
Liu, Jiping  
et al.

### Publication Date

2020-08-11





### DOI

10.1073/pnas.1918883117

Peer reviewed



# Single-cell RNA-seq analysis revealed long-lasting adverse effects of tamoxifen on neurogenesis in prenatal and adult brains

Chia-Ming Lee<sup>a,1</sup> , Liqiang Zhou<sup>b,1</sup> , Jiping Liu<sup>b</sup>, Jiayu Shi<sup>b</sup>, Yanan Geng<sup>b</sup>, Min Liu<sup>a</sup>, Jiaruo Wang<sup>a</sup>, Xinjie Su<sup>a</sup>, Nicholas Barad<sup>a</sup>, Junbang Wang<sup>b</sup>, Yi Eve Sun<sup>a,b,2</sup> , and Quan Lin<sup>a,2</sup> 

<sup>a</sup>Department of Psychiatry and Behavioral Sciences, Intellectual Development and Disabilities Research Center, University of California, Los Angeles, CA 90095; and <sup>b</sup>Stem Cell Translational Research Center, Tongji Hospital, Tongji University School of Medicine, Shanghai 200092, China

Edited by Arturo Alvarez-Buylla, University of California, San Francisco, and accepted by Editorial Board Member Yuh Nung Jan June 30, 2020 (received for review October 29, 2019)

**The CreER/LoxP system is widely accepted to track neural lineages and study gene functions upon tamoxifen (TAM) administration. We have observed that prenatal TAM treatment caused high rates of delayed delivery and fetal mortality. This substance could produce undesired results, leading to data misinterpretation. Here, we report that administration of TAM during early stages of cortical neurogenesis promoted precocious neural differentiation, while it inhibited neural progenitor cell (NPC) proliferation. The TAM-induced inhibition of NPC proliferation led to deficits in cortical neurogenesis, dendritic morphogenesis, synaptic formation, and cortical patterning in neonatal and postnatal offspring. Mechanistically, by employing single-cell RNA-sequencing (scRNA-seq) analysis combined with in vivo and in vitro assays, we show TAM could exert these drastic effects mainly through dysregulating the Wnt-Dmrta2 signaling pathway. In adult mice, administration of TAM significantly attenuated NPC proliferation in both the subventricular zone and the dentate gyrus. This study revealed the cellular and molecular mechanisms for the adverse effects of TAM on corticogenesis, suggesting that care must be taken when using the TAM-induced CreER/LoxP system for neural lineage tracing and genetic manipulation studies in both embryonic and adult brains.**

tamoxifen | CreER | LoxP | Wnt | Dmrta2

The tamoxifen (TAM)-inducible CreER/LoxP system is one of the most widely used genetic tools that have enabled precise gene manipulation in distinct cell subpopulations at any specific time point. Besides gene knockout, CreER/LoxP technology has also enabled labeling of any cell types for genetic fate-mapping study (1–4). TAM, a selective estrogen receptor modulator, is considered a pioneering and commonly used drug to treat estrogen receptor positive breast cancer (5). In humans, a study based on the AstraZeneca Safety Database suggested that TAM therapy of breast cancer during pregnancy is tightly associated with spontaneous abortions, fetal defects, and congenital malformations (6). To avoid significant birth defects, TAM administration needs to be discontinued during pregnancy in breast cancer patients (7–9). In rodents, adverse effects of TAM on prenatal and postnatal mice have been reported by a considerable number of studies. Empirically, administration of TAM or its active metabolite, 4-hydroxytamoxifen (4-OH-TAM) by either oral gavage (~1.5 to 10 mg TAM/mouse) or intraperitoneal (IP) injections (~750 µg to 1.5 mg TAM/mouse) to pregnant mice led to embryonic lethality and/or dystocia. To obtain postnatal offspring, it is frequently required to perform a caesarian section followed by fostering (10–15).

Our initial study showed that administration of TAM to pregnant mice at embryonic day 10 (E10) reduced the size of the cerebral hemispheres and the olfactory bulbs, enlarged the lateral ventricle, and thinned the cortical plate (Fig. 1A), suggesting prenatal TAM exposure has a drastic impact on cortical neurogenesis. We administered TAM to more than 70 litters of three

different mouse lines by IP injection (i.e., C57BL/6, 129S6/C57BL/6, and CD1). TAM doses tested per pregnant dam were 500 µg (5 litters), 750 µg (≥50 litters), 1 mg (5 litters), and 2 mg (≥10 litters). Delayed delivery and/or fetal mortality were always observed in litters with a dose of 750 µg/animal and above.

To examine the effects of TAM on cortical neurogenesis, we carried out single-cell RNA-sequencing (scRNA-seq) analysis. Combined with quantitative in situ hybridization (ISH) and immunostaining assays, we found a single dose, prenatal TAM administration promoted precocious neuronal differentiation, while it blocked neural progenitor cell (NPC) proliferation which ultimately resulted in impaired cortical neurogenesis in prenatal and perinatal brains. We further revealed that TAM could exert these adverse effects via dysregulating Wnt-Dmrta2 signaling, which has been shown to play critical roles in NPC fate maintenance and neural differentiation (16, 17). Moreover, we showed that TAM administration at E8.5 severely impaired neurogenesis, dendritic morphogenesis, synaptic density, and gliogenesis in

## Significance

The tamoxifen (TAM)-inducible CreER/LoxP system is one of the most widely used genetic tools that have enabled precise gene manipulation in distinct cell subpopulations at any specific time point and labeling of any cell types for genetic fate mapping. We report that administration of TAM during early stages of cortical neurogenesis inhibits neural progenitor cell proliferation and impaired cortical neurogenesis, dendritic morphogenesis, synaptic density, and gliogenesis in postnatal offspring. By employing single-cell RNA sequencing analysis combined with in vivo and in vitro assays, we found TAM could exert these drastic effects through dysregulating the Wnt-Dmrta2 signaling pathway. This study shows that care must be taken when using the TAM-induced CreER/LoxP system for neural lineage tracing and genetic manipulation studies.

Author contributions: C.-M.L., L.Z., Y.E.S., and Q.L. designed research; C.-M.L., L.Z., J.L., J.S., Y.G., M.L., Jiaruo Wang, X.S., N.B., Junbang Wang, and Q.L. performed research; Q.L. analyzed data; and C.-M.L., L.Z., and Q.L. wrote the paper.

The authors declare no competing interest.

This article is a PNAS Direct Submission. A.A.-B. is a guest editor invited by the Editorial Board.

Published under the PNAS license.

Data deposition: The sequences reported in this paper have been deposited in Gene Expression Omnibus (GEO) database, <https://www.ncbi.nlm.nih.gov/geo/> (accession no. GSE152125).

<sup>1</sup>C.-M.L. and L.Z. contributed equally to this work.

<sup>2</sup>To whom correspondence may be addressed. Email: [ysun@mednet.ucla.edu](mailto:ysun@mednet.ucla.edu) or [qlin@mednet.ucla.edu](mailto:qlin@mednet.ucla.edu).

This article contains supporting information online at <https://www.pnas.org/lookup/suppl/doi:10.1073/pnas.1918883117/-DCSupplemental>.

First published July 29, 2020.

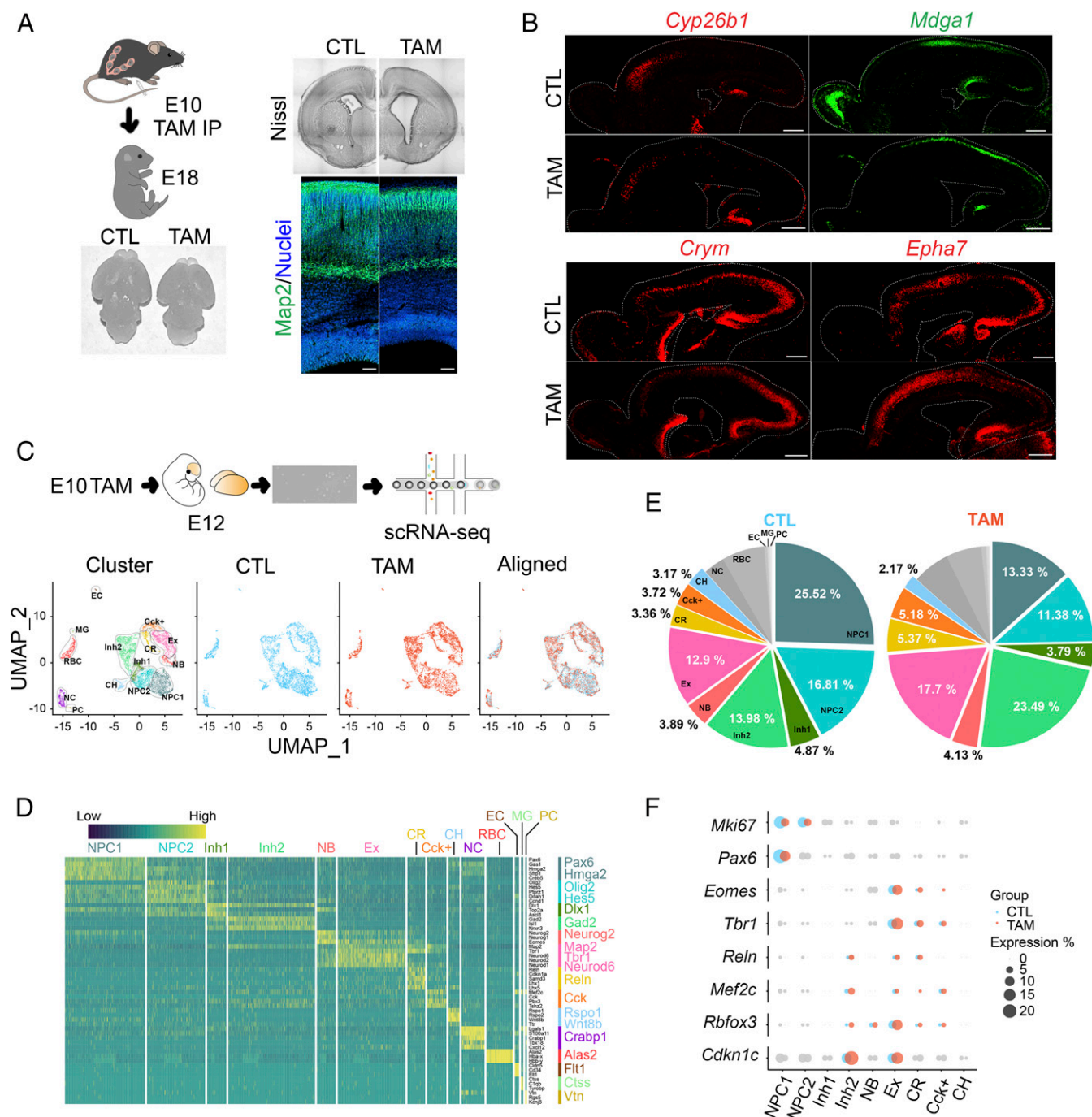


**Fig. 1.** Prenatal TAM exposure impaired cortical neurogenesis. (A) TAM was injected into pregnant mice at E10 (750  $\mu$ g/animal). The brains were removed at E18. TAM treatment reduced the size of the cerebral hemispheres and the olfactory bulbs. Nissl staining showed an enlargement of the lateral ventricles (*Upper Right*). Map2 immunostaining shows TAM treatment at E10 dramatically thinned cortical plate at E18 (*Lower Right*). CTL, oil control; TAM, tamoxifen treated; Map2, microtubule associated protein 2. (Scale bar, 50  $\mu$ m.) (B) Prenatal TAM exposure at E10 altered cortical area patterning at E18 in the motor cortex (*Cyp26b1* and *Epha7*), the somatosensory cortex (*Mdga1*), and the visual cortex (*Crym* and *Epha7*). *Cyp26b1*, cytochrome P450 family 26 subfamily b member 1; *Epha7*, EPH receptor a7; *Mdga1*, MAM domain containing glycosylphosphatidylinositol anchor 1; *Crym*, Crystallin Mu. (Scale bar, 400  $\mu$ m.) (C) Schematic overview of single-cell isolation and scRNA-seq. Visualization of single-cell data by UMAP plot of clustering of E12 cells. NPC1, cortical neural progenitor cells; NPC2, subcortical neural progenitor cells; Inh1, inhibitory neurons (mainly derived from the medial ganglionic eminence [MGE]); Inh2, inhibitory neurons (mainly derived from the lateral ganglionic eminence [LGE] or the caudal ganglionic eminence [CGE]); NB, neuroblasts; Ex, excitatory neurons; Cck+, Cck<sup>+</sup> cells; CR, Cajal-Retzius cells; CH, cortical hem cells; NC, neural crest cells; RBC, red blood cells; EC, endothelial cells; MG, microglia; PC, pericytes. (D) Heatmap shows top cell-type-specific genes expressed in the clusters defined in C. The representative genes of each cluster are listed on the *Right*. (E) Pie chart shows major cell-type percentages between CTL and TAM groups. (F) Patterning analysis of cell fate and cell cycle markers. Circles represent fractions of positive cells in each cluster. Mki67, marker of proliferation K<sub>i</sub>-67; Pax6, paired box 6; Eomes, eomesodermin; Tbr1, T-box brain transcription factor 1; Reln, reelin; Mef2c, myocyte enhancer factor 2C; Rbfox3, RNA binding Fox-1 homolog 3; Cdkn1c, cyclin dependent kinase inhibitor 1C.

postnatal offspring. In adult mice, TAM treatment dramatically attenuated neural stem cell proliferation in the subventricular zone (SVZ) and the dentate gyrus (DG), the two areas where adult neurogenesis occurs.

## Results

**Prenatal TAM Administration Impaired Neurogenesis and Cortical Organization in Perinatal Offspring.** It has been shown that the highest tolerable dose for a single prenatal (E7.5 to E10.5) TAM IP injection without significant lethality at term is about 1 mg per pregnant dam (~30 to 60  $\mu\text{g}$  TAM per gram body weight) (15, 18). Our preliminary study showed administration of 500  $\mu\text{g}$  TAM to Prominin1 CreER reporter mice (Prom1-CreER/floxed ZsGreen) at E8.5 and E10 did not elicit detectable green fluorescent protein signal at E18. Therefore, to study the effects of TAM on corticogenesis, we administered 750  $\mu\text{g}$  of TAM per pregnant dam (~25 to 30  $\mu\text{g}$  TAM per gram body weight).

To study the effects of TAM on cortical neurogenesis, we administered TAM to pregnant dams at E10, the time when cortical neurogenesis begins in the forebrain (19). We found TAM dysregulated the expression of multiple cortical patterning genes in the motor cortex (*Cyp26b1* and *Epha7*), the somatosensory cortex (*Mdga1*), and the visual cortex (*Cym* and *Epha7*) in E18 offspring (Fig. 1B). TAM treatment somewhat reduced visual cortex marker gene expression and expanded the somatosensory gene *Mdga1* expression posteriorly, implying cortical patterning deficits in TAM-treated offspring.

For single-cell RNA sequencing, TAM was administered to the pregnant dam at E10. To minimize potential variability between individuals, we pooled left and right hemispheres isolated from different litters per experimental condition. At E12 when neuronal polarity has not been fully established, tissue dissection and cell dissociations steps have little effects on cell integrity (cell viability >95%). The pooled samples were subjected to droplet-based scRNA-seq analysis (10 $\times$  Genomics) (Fig. 1C). We then subset the datasets (4,193 cells/condition set.seed = 3) and applied quality filter and integrated analysis to merge control (CTL) and TAM datasets with a total of 8,386 cells and 17,071 genes using the Seurat package (20, 21). Based on uniform manifold approximation and projection (UMAP) analysis, we segregated the cells into 14 clusters (Fig. 1C). According to gene expression enrichment, we annotated 14 clusters. There are neural progenitor cells (NPC1, *Pax6* and NPC2, *Olig2*), inhibitory neurons (*Inh1*, *Dlx1* and *Inh2*, *Gad2*), cortical neuroblasts (NB, *Neurog2*), cortical excitatory neurons (Ex, *Neurod6*), Cajal-Retzius cells (CR, *Reln*), cortical *Cck*<sup>+</sup> neurons (*Cck*<sup>+</sup>, *Cck*), cortical hem neurons (CH, *Rspo1*), neural crest cells (NC, *Crabp1*), red blood cells (RBC, *Alas2*), endothelial cells (EC, *Fli1*), microglia (MG, *Ctss*), and pericytes (PC, *Vtn*) (Fig. 1D).

To assess the overall effect of TAM on cell fate specification, we calculated the ratios of cells in each cluster over total analyzed cells. We found that prenatal TAM exposure greatly reduced the ratio of cortical and subcortical NPCs (NPC1 and NPC2, small blue and blue color) by 17.62%, while it caused a total of 16.7% increase in cortical (Ex, pink color) and subcortical (*Inh1* and *Inh2*, darkgreen and green color) neurons, CR cells (dark yellow color), and *Cck*<sup>+</sup> neurons (orange color) (Fig. 1E). Prenatal TAM treatment also reduced the ratio of cells in one of the major brain patterning centers, the cortical hem (light blue color) (22). To save computational recourse, we randomly subset the CTL and TAM dataset to 4,193 cells/condition (23). We tested cell subtype composition using two other random subset parameters (set.seed = 5 and 25). We found that the cell type compositions are similar among the three random subset and the total cell datasets (SI Appendix, Fig. S1A). We did not observe cell cluster loss due to random subset in the current study. Next, we analyzed the expression of cell fate markers in neuronal lineage clusters. In TAM-treated brains, the numbers

of proliferating cells (*Mki67*<sup>+</sup>) and cortical ventricular zone (VZ) NPCs (*Pax6*<sup>+</sup>, NPC1 cluster) were notably reduced, while the number of *Eomes* expressing cells was increased. The increased *Eomes*<sup>+</sup> cells mainly resided in the newborn cortical neuron cluster (Ex), implying that TAM treatment promoted *Eomes*<sup>+</sup> SVZ progenitors to express neuronal genes precociously. In line with the findings above, the number of cells expressing neuronal genes, such as *Reln*, *Tbr1*, *Rbfox3*, and *Mef2c*, was increased in cortical neuron clusters (Ex, *Cck*<sup>+</sup>, and CR) of TAM-treated brains. Moreover, increased parvalbumin interneuron precursors (*Mef2c*<sup>+</sup>) in the *Inh2* cluster further suggested a precocious neurogenesis in TAM-treated brains (24). Importantly, there were more cells in *Inh2* and Ex clusters expressing the cell cycle G1 phase marker, *Cdkn1c* in TAM-treated brains (Fig. 1F). Cyclin-dependent kinase inhibitor 1C (*Cdkn1c*) is a strong inhibitor of several G1 cyclin/Cdk (cyclin-dependent kinases) complexes and a negative regulator of cell proliferation (25, 26). Increased number of cells in the G1 phase suggests an early cell cycle withdrawal and subsequent advanced cortical neuronal differentiation. Taken together, our initial scRNA-seq analysis suggested biphasic effects of TAM on cortical neurogenesis. On one hand, TAM suppressed cell cycle progression and inhibited NPC proliferation; on the other hand, it increased the number of SVZ progenitors expressing neuronal genes, and thus led to precocious neuronal differentiation.

**Prenatal TAM Exposure Inhibited VZ Progenitor Proliferation.** To validate the initial scRNA-seq analysis, we first measured the expression of NPCs in the cortex using the VZ and the SVZ markers, *Pax6* and *Eomes*, respectively. TAM was IP injected at E10. Brain samples were collected at E12. Immunostaining assay showed that in TAM-treated brains, the number of *Pax6*<sup>+</sup> NPCs was significantly reduced (CTL = 87  $\pm$  4%, TAM = 76  $\pm$  5%; mean  $\pm$  SD), while *Eomes*<sup>+</sup> cells in the SVZ were slightly increased (CTL = 8  $\pm$  3%, TAM = 12  $\pm$  3%; mean  $\pm$  SD) (Fig. 2A). Quantitative ISH assay showed the average number of *Pax6* mRNA puncta reduced from 7  $\pm$  2/cell in CTL to 5  $\pm$  1/cell in the TAM-treated cortex. The average number of *Eomes* puncta increased from 3  $\pm$  0.8/cell to 5  $\pm$  1.6/cell (mean  $\pm$  SD) in TAM brains (Fig. 2B). Second, BrdU incorporation assay combined with *Mki67* immunostaining showed that TAM exposure at E10 greatly reduced the number of cells in the cell cycle and in the S phase (BrdU: CTL = 36  $\pm$  8%, TAM = 26  $\pm$  6% and *Mki67*: CTL = 35  $\pm$  6%, TAM = 24  $\pm$  6%; mean  $\pm$  SD) (Fig. 2C). We observed similar results when TAM was administered at the peak of cortical neurogenesis (SI Appendix, Fig. S1B). Third, we measured cell cycle S phase length using a 5-ethynyl-2'-deoxyuridine (EdU)/BrdU double labeling paradigm (25) (Fig. 2D). Cells that left the S phase during the labeling period (2 h) were labeled with EdU only (green color). Cells in S phase were labeled with BrdU (red color). The EdU/BrdU double labeling assay showed a prolonged S phase in TAM-treated, proliferating NPCs (CTL = 4  $\pm$  1 h, TAM = 7  $\pm$  2 h; mean  $\pm$  SD) (Fig. 2D). Fourth, we assessed the number of dividing cells (M phase) in the cortex using phospho-Histone H3 (pH3) antibody (26). We found there were more basal pH3<sup>+</sup> cells in TAM-treated brains than in the control (CTL = 0.4  $\pm$  0.3%, TAM = 1  $\pm$  0.5%; mean  $\pm$  SD), which may cause the transient increase of *Eomes*<sup>+</sup> cells. Contrary to its effect on basal dividing cells, TAM reduced the number of pH3<sup>+</sup> apical dividing cells (CTL = 6  $\pm$  1.4%, TAM = 4  $\pm$  0.8%; mean  $\pm$  SD) (Fig. 2E), which may cause the reduction of *Pax6*<sup>+</sup> NPCs and lead to neurogenesis impairment. Finally, we found TAM treatment at early (E10) and midstage (E13) of cortical development quickly increased the expression level of the cell cycle arrest molecule, *Cdkn1c* (CTL = 0.2  $\pm$  0.04 puncta/cell, TAM = 0.4  $\pm$  0.07 puncta/cell; mean  $\pm$  SD) (Fig. 2F and SI Appendix, Fig. S1C). Taken together, it appeared that TAM administration disrupted cell cycle progression which in turn inhibited NPC proliferation. Simultaneously, TAM promoted transient



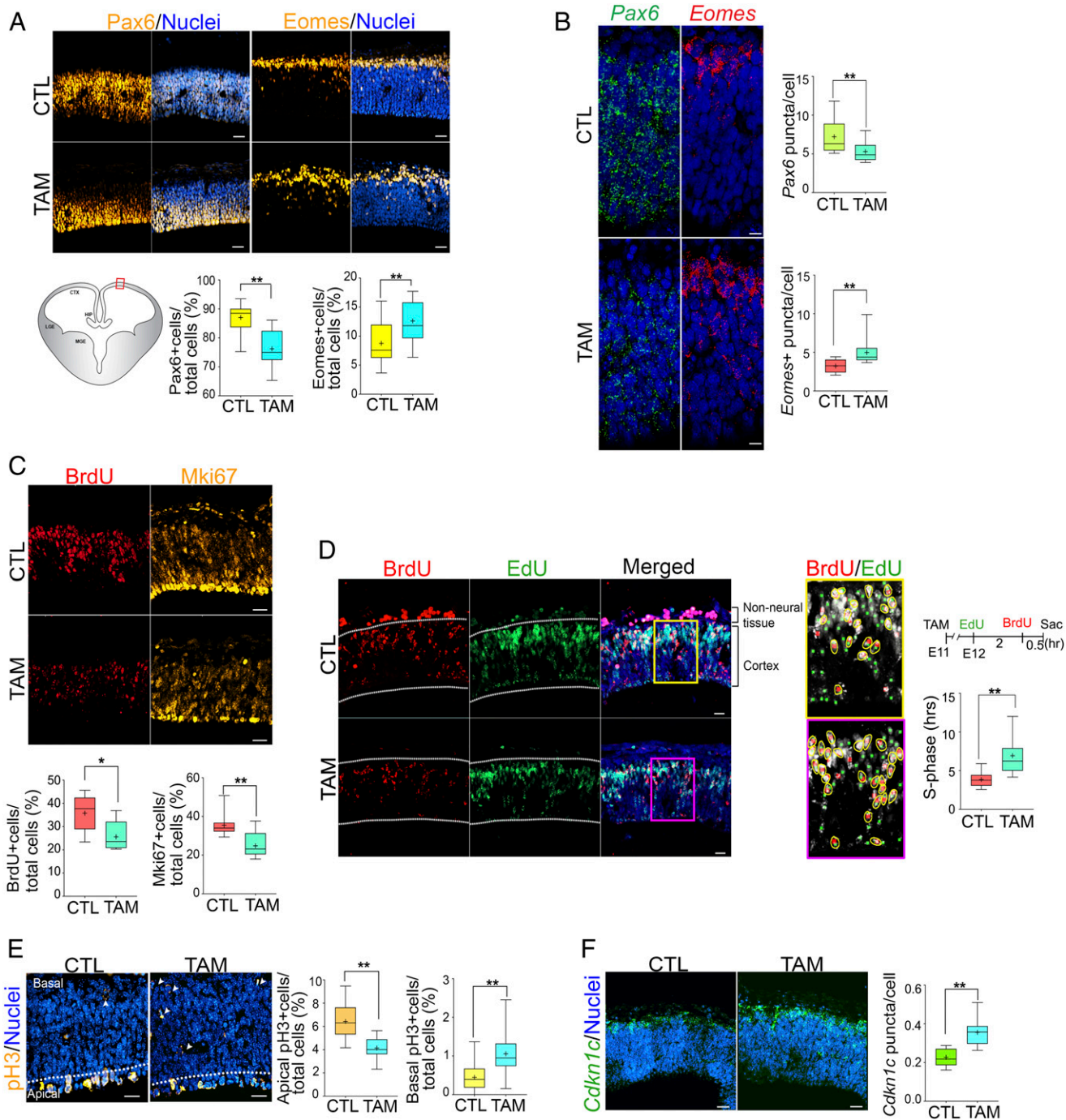


**Fig. 2.** Prenatal TAM administration inhibited neural progenitor proliferation. (A) Pax6 and Eomes immunostaining shows TAM treatment at E10 significantly inhibited VZ progenitor proliferation at E12, while it increased the number of cells in the SVZ (Pax6<sup>+</sup> cells,  $P < 0.0001$ ; Mann–Whitney  $U$  test, CTL  $n = 24$ , TAM  $n = 27$ ). (Scale bar, 30  $\mu$ m.) The red box in the *Lower Left* diagram shows the region used for quantification analysis. *Lower Right* shows the percentage of Pax6<sup>+</sup> or Eomes<sup>+</sup> cells over total cells. CTX, cortex; HIP, hippocampus; LGE, lateral ganglionic eminence; MGE, medial ganglionic eminence. The box plot shows the minimum, the maximum, the median, the mean (the + symbol), and the first and the third quartiles. (B) ISH shows administration of TAM at early brain development (E10) reduced the expression and the number of VZ progenitors (Pax6<sup>+</sup>), while it increased the expression of Eomes and the number of SVZ progenitors (Eomes<sup>+</sup>) (Pax6 puncta/cell,  $P = 0.0026$ ; Eomes puncta/cell,  $P = 0.0002$ ; Mann–Whitney  $U$  test, CTL  $n = 14$ , TAM  $n = 19$ ). (Scale bar, 10  $\mu$ m.) (C) TAM dramatically reduced numbers of cells in S phase (BrdU<sup>+</sup>) and total cells in the cell cycle (Mki67<sup>+</sup>) (BrdU,  $P = 0.0264$ ; Mki67,  $P = 0.0007$ ; Mann–Whitney  $U$  test, CTL  $n = 19$ , TAM  $n = 18$ ). TAM was administered at E10. BrdU was injected to the pregnant dam at E12. Samples were collected 30 min after BrdU administration. (Scale bar, 30  $\mu$ m.) (D) Kinetic analysis of S phase cell cycle progression ( $P < 0.0001$ , Mann–Whitney  $U$  test, CTL  $n = 20$ , TAM  $n = 21$ ). TAM was administered at E11. EdU was injected at E12. BrdU was injected 2 h after EdU administration. The brains were collected 30 min after EdU injection. The enlarged images on the *Right* show quantification of BrdU (red color) single or double positive cells. The Edu/BrdU double positive cells were labeled with yellow ovals. (Scale bar, 20  $\mu$ m.) The broken lines label the cortex. (E) TAM administration increased the number of basal dividing cells (phospho-Histone H3<sup>+</sup>), while it reduced the number of apical dividing cells (apical,  $P < 0.0001$ ; basal,  $P < 0.0001$ ; Mann–Whitney  $U$  test, CTL  $n = 32$ , TAM  $n = 38$ ). (Scale bar, 20  $\mu$ m.) (F) *Cdkn1c* ISH shows prenatal administration of TAM at E10 detained cells in G1 phase ( $P < 0.0001$ , Mann–Whitney  $U$  test, CTL  $n = 12$ , TAM  $n = 12$ ). (Scale bar, 30  $\mu$ m.) \*,  $0.01 \leq P < 0.05$ ; \*\* $P < 0.01$ .

SVZ progenitor proliferation followed by early cell cycle withdrawal, which led to precocious neurogenesis. Although we cannot rule out the possibility that reduced BrdU signal in TAM-treated NPCs was due to DNA repair, the result of BrdU incorporation assay was consistent with Mki67, pH3, Pax6, and Eomes quantification analyses.

To rule out the possibility that the reduction in the number of NPCs was due to TAM-induced apoptosis, we carried out terminal deoxynucleotidyl transferase dUTP nick-end labeling (TUNEL) assay. We did not detect increased apoptosis in E12 brains when TAM (2 mg/animal) was administered to pregnant mice at E10 (SI Appendix, Fig. S1D).

**TAM Promoted Precocious and Transient Neuronal Differentiation in Prenatal Brains.** The scRNA-seq analysis showed an increased number of cells expressing postmitotic neuronal markers, such as *Reln*, *Rbfox3*, *Tbr1*, and *Mef2c* at E12 when TAM was administered at E10. There was an increased number of cells expressing cell cycle G1 phase gene *Cdkn1c* in TAM-treated brains, which further suggested precocious neural differentiation. In agreement with the analyses above, the immunostaining assays showed that TAM exposure at E10 greatly promoted the production of not only early-born, *Reln*<sup>+</sup> Cajal-Retzius cells and *Tbr1*<sup>+</sup> deep layer neurons (*Reln*: CTL = 1.7 ± 0.5%, TAM = 2.5 ± 0.6% and *Tbr1*: CTL = 9 ± 1.7%, TAM = 13 ± 1.6%; mean ± SD) (Fig. 3A and B), but also *Mef2c*<sup>+</sup> superficial layer cells at E12 (CTL = 0.5 ± 0.3%, TAM = 1.9 ± 0.5%; mean ± SD) (Fig. 3C) (19). The increased *Mef2c*-expressing cells in the cortex were probably from the *Cck*<sup>+</sup> cluster (Fig. 1F). The above immunostaining results were further confirmed by ISH assay using a pan-neuronal marker, *Rbfox3* (CTL = 0.16 ± 0.04 puncta/cell, TAM = 0.20 ± 0.05 puncta/cell; mean ± SD) (Fig. 3D). Moreover, we also showed that TAM treatment at the peak of cortical neurogenesis (E13) dramatically increased *Tbr1*<sup>+</sup> and *Mef2c*<sup>+</sup> cells in the cortical plate at E14, while having little effects on the total number of *Reln*<sup>+</sup> cells in the cortical marginal zone (MZ) (SI Appendix, Fig. S24). This may be because *Reln*<sup>+</sup> cells are one type of the earliest born cortical neurons which have differentiated before TAM administration (27).

**The Long-Lasting Effects of Prenatal TAM Exposure in Postnatal Offspring.** To evaluate the potential long-lasting effects of TAM exposure on cortical neurogenesis, we injected TAM to pregnant dams preceding neural tube closure (E8.5) and examined cortical neurogenesis at E18 and at postnatal day 30 (P30). TAM treatment dramatically reduced the thickness of the cortical plate (Map2: CTL = 478 ± 40 μm, TAM = 355 ± 32 μm; mean ± SD) and the number of cortical neurons in E18 offspring (*Rbfox3*: CTL = 54 ± 7%, TAM = 41 ± 11%; mean ± SD) and in P30 offspring (*Rbfox3*: CTL = 65 ± 5%, TAM = 58 ± 3% and *Tbr1*: CTL = 57 ± 5%, TAM = 43 ± 3%; mean ± SD) (Fig. 3E and F). In the hippocampus, prenatal TAM treatment also caused subtle reduction of cell numbers in the CA1 and the DG (SI Appendix, Fig. S2B). Strikingly, administration of TAM at E8.5 severely impaired apical dendritic complexity in P30 brains, especially in the cortical marginal zone (CTL = 1.3 ± 0.3 dendritic fragments/μm<sup>3</sup>, TAM = 0.8 ± 0.013 dendritic fragments/μm<sup>3</sup>; mean ± SD) (Fig. 3G). Moreover, the synaptic density was reduced in TAM-treated cortex (CTL = 0.15 ± 0.06 puncta/μm<sup>2</sup>, TAM = 0.06 ± 0.03 puncta/μm<sup>2</sup>; mean ± SD) (Fig. 3H). Administration of TAM at E13 (the peak period of cortical neurogenesis) to an outbred mouse strain (CD1) and a transgenic mouse line (Prom1-CreER/ZsGreen) also showed reduced number of cortical neurons (SI Appendix, Fig. S2C and D), suggesting TAM treatment has long-lasting effects on cortical neurogenesis regardless of the genetic backgrounds.

In addition to cortical neurogenesis, in E8.5 TAM-treated P30 offspring, our data showed a significant reduction in the percentage of *Olig2*<sup>+</sup> oligodendrocytes in the corpus callosum defined by *Cnp*

and *Mbp* staining. Compared to the control, *Cnp* and *Mbp* immunostaining showed TAM treatment caused irregular axon bundle organization and severely reduced the expansion of the corpus callosum, where the commissural fibers connect left and right hemispheres (SI Appendix, Fig. S3A). We observed a statistically nonsignificant reduction in the number of *Gfap*<sup>+</sup> astrocytes in the corpus callosum, while the number of *Aldoc*<sup>+</sup> astrocytes remained unchanged in the cortex (SI Appendix, Fig. S3B and C).

**Prenatal TAM Exposure Perturbed Wnt Signaling Which Has Been Shown to Strongly Correlate with Neural Progenitor Maintenance, Differentiation, and Cortical Patterning.** To reveal the underlying molecular mechanisms, we carried out gene regulatory network analysis of NPCs and cortical hem cells using the bigSCale2 toolkit to identify hub genes that TAM used to manipulate corticogenesis (28). We chose to analyze NPC1/2 and CH clusters because of the tight association between VZ NPC proliferation and cortical neurogenesis. The cortical hem, one of the main brain patterning organizers, has been shown to regulate cortical patterning (22, 29).

We discovered four major network modules in CTL- and three modules in TAM-treated cells (Fig. 4A, Left). Compared with the CTL, the TAM network showed lower edges to node density (CTL = 6.89, TAM = 4.92) and modularity (CTL = 0.61, four modules, TAM = 0.29, three modules), suggesting the CTL network preserved a stronger intramodular connectivity and higher gene expression heterogeneity. Gene ontology (GO) enrichment analysis showed the four modules in the CTL comprised of genes mainly related to forebrain development, cell division, cell cycle progression, and ribonucleoprotein complex biogenesis (Fig. 4A, Upper Right). Compared to the CTL, TAM treatment reduced the GO enrichments to three modules composed of genes related to projection assembly and Wnt signaling, cell division, and ribonucleoprotein complex biogenesis (Fig. 4A, Lower Right). Cell cycle progression genes were not GO enriched in the TAM-treated sample, suggesting the expression of genes that control cell cycle progression was largely dysregulated. Closer inspection revealed the pagerank centrality of differentially expressed hub genes (orange-red color and blue color) was reduced in a random pattern within the gene regulatory network of TAM-treated NPCs and CH cells (Fig. 4A, Left). One of the most striking examples is the forebrain development module. The regulatory networks of the hub genes in this module, such as *Dmrta2*, *Wnt8b*, *Emx2*, and *Dmrt3*, were greatly altered in TAM-treated cells. Directly connected genes (nodes) to *Dmrta2* and *Wnt8b* were reduced from 62 in CTL to 17 in TAM-treated cells, and from 109 to 57, respectively, indicating weakened gene-gene interactions in TAM-treated cells. These hub genes are critical components of multiple pathways that regulate neural progenitor maintenance, cortical neurogenesis, and cortical patterning (i.e., Wnt, BMP, and Notch pathways) (17, 22).

Intriguingly, a recent study by Young et al. showed that *Dmrta2*, a novel Wnt-dependent transcription factor, regulated *Hes1* and other proneural genes to maintain NPC fate (17). *Emx1*-Cre conditional knockout of *Dmrta2* accelerated cell cycle exit, increased *Eomes*<sup>+</sup> cells, and promoted transient neuronal differentiation. In line with this evidence, an earlier study by Nakamura et al. showed that *Hes1* null mice exhibited premature progenitor cell differentiation and reduction of multipotent progenitors' self-renewal activity (16). These phenotypes somewhat resemble our findings in TAM-treated brains. scRNA-seq analysis showed that the expression levels of *Wnt8b*, *Dmrta2*, a *Dmrta2* downstream target *Hes1*, a Wnt receptor subunit, *Lrp6*, and a Bmp receptor subunit, *Avcr2b*, were decreased in the TAM-treated NPCs and/or CH cells (Fig. 4B). Our ISH assays show that TAM treatment at E10 dramatically down-regulated expression levels of *Wnt8b*, *Lrp6*, *Dmrta2*, *Hes1*, and *Avcr2b* in the cortex at E12 (average puncta/cell, *Wnt8b*: bin1, CTL = 4.7 ± 0.30, TAM = 3.5 ± 0.16; bin2, CTL = 4.7 ± 0.18, TAM = 3.4 ± 0.20; bin8,



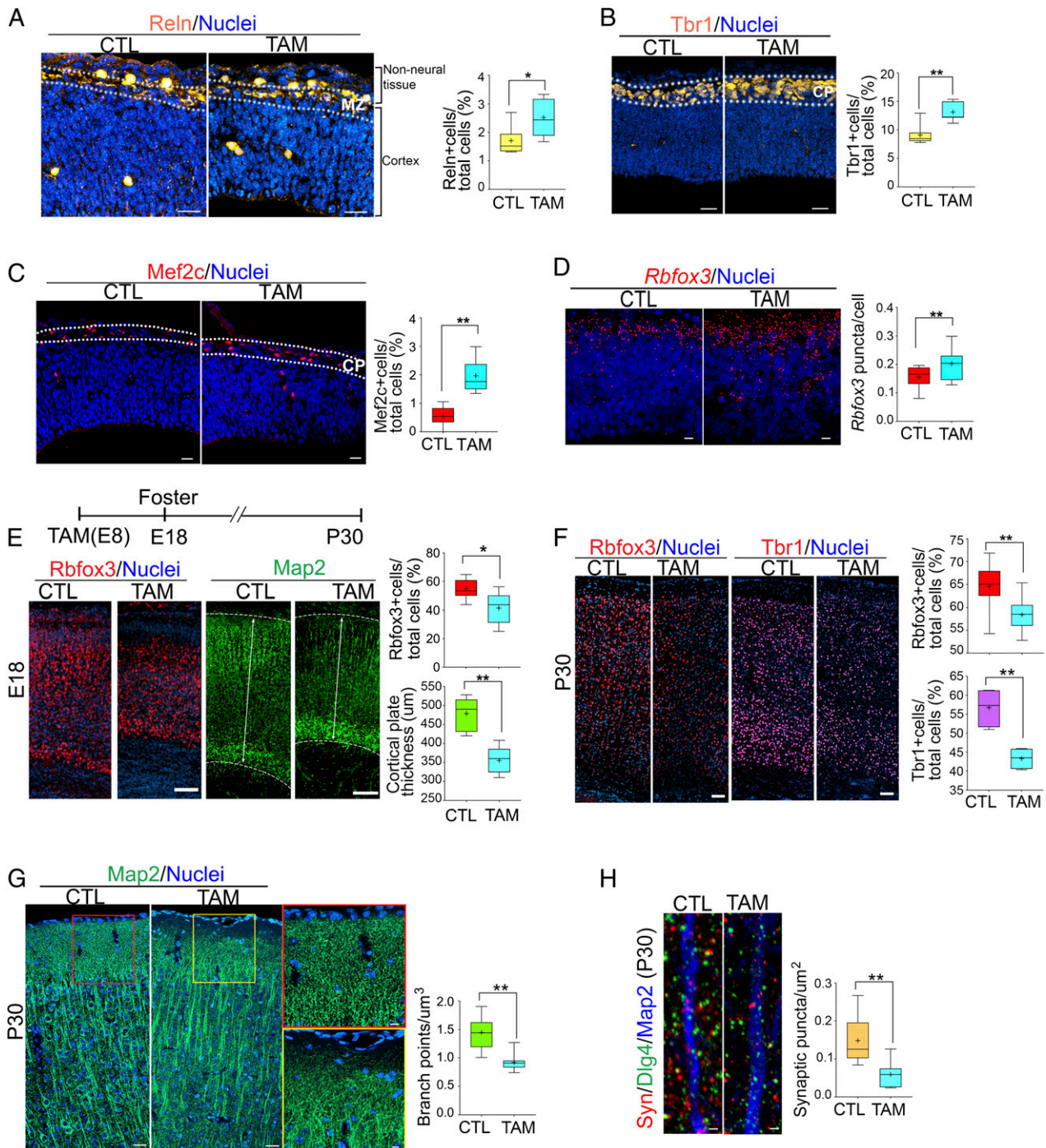


**Fig. 3.** Prenatal TAM administration promotes precocious neurogenesis and has long-lasting effects on corticogenesis in postnatal offspring. (A–D) Administration of TAM at E10 increased numbers of Reelin (ReIn) positive, Cajal–Retzius cells at E12 ( $P = 0.0115$ , Mann–Whitney  $U$  test, CTL  $n = 7$ , TAM  $n = 9$ ) (Scale bar, 30  $\mu\text{m}$ .), Tbr1<sup>+</sup> neurons ( $P = 0.0037$ , Mann–Whitney  $U$  test, CTL  $n = 8$ , TAM  $n = 7$ ) (Scale bar, 30  $\mu\text{m}$ .), and Mef2c<sup>+</sup> superficial layer neurons ( $P < 0.0001$ , Mann–Whitney  $U$  test, CTL  $n = 20$ , TAM  $n = 20$ ) (Scale bar, 20  $\mu\text{m}$ .). ISH assay shows prenatal TAM exposure at E10 transiently increased the total number of Rbfox3<sup>+</sup> postmitotic neurons at E12 ( $P = 0.0354$ , Mann–Whitney  $U$  test, CTL  $n = 10$ , TAM  $n = 10$ ) (Scale bar, 10  $\mu\text{m}$ .). The broken lines label the marginal zone (MZ) (A) or the cortical plate (CP) (B and C). (E) TAM was administered at E8.5. Cortical neurons were significantly reduced in E18 brains (Rbfox3,  $P = 0.0262$ , Mann–Whitney  $U$  test, CTL  $n = 17$ , TAM  $n = 18$ . Map2,  $P < 0.0001$ , Mann–Whitney  $U$  test, CTL  $n = 20$ , TAM  $n = 35$ ). (F) TAM exposure at E8.5 impaired cortical neurogenesis in P30 offspring (Rbfox3,  $P < 0.0001$ , Mann–Whitney  $U$  test, CTL  $n = 15$ , TAM  $n = 18$ . Tbr1,  $P = 0.0286$ , Mann–Whitney  $U$  test, CTL  $n = 9$ , TAM  $n = 9$ ). (Scale bar, 100  $\mu\text{m}$ .) (G) TAM treatment decreased dendrite complexity in P30 offspring. Dendritic morphology was quantified using Imaris filament function; statistics denoted the number of branching points ( $P = 0.0002$ , Mann–Whitney  $U$  test, CTL  $n = 9$ , TAM  $n = 9$ ). The *Right* shows enlarged view of the box areas in the *Left* two panels and the surface model for dendrite quantification. (Scale bar, 20  $\mu\text{m}$ .) (H) Prenatal TAM administration (E8.5) altered synaptic formation in adult offspring. Presynaptic terminals were identified by synapsin staining (red color). Postsynaptic structures were identified by discs large MAGUK scaffold protein 4 (Dlg4 [PSD95]) staining (green color). Dendrites were labeled by Map2 staining (blue color). Synapses were identified by the close proximity of pre- and postsynaptic elements ( $\leq 1 \mu\text{m}$ ) ( $P = 0.0004$ , Mann–Whitney  $U$  test, CTL  $n = 10$ , TAM  $n = 10$ ). (Scale bar, 1  $\mu\text{m}$ .) \*,  $0.01 \leq P < 0.05$ ; \*\* $P < 0.01$ .

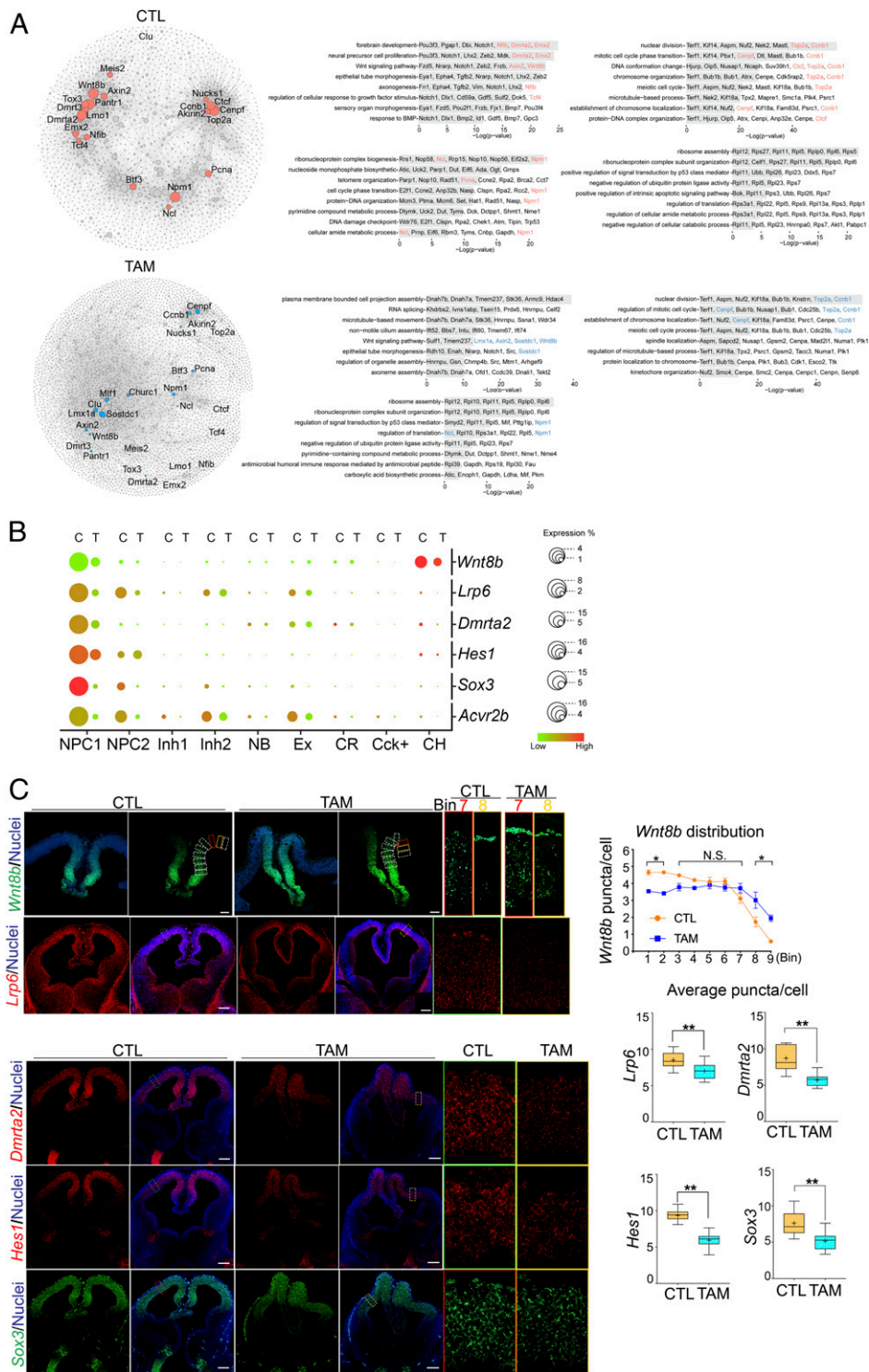


**Fig. 4.** Prenatal TAM administration perturbed *Dmrt2*-*Hes1*, *Wnt*, and *Bmp* signaling pathways. (A) The *Left* shows CTL and TAM gene regulatory network analysis of scRNA-seq of NPC and CH clusters. The node size is proportional to its pagerank centrality. Orange-red (CTL) and blue (TAM) dots show genes in the intersection of three gene sets: 1) Top 200 differentially expressed genes identified using Seurat package *FindAllMarkers* function between CTL and TAM; 2) Top 200 genes with the biggest change in pagerank absolute value between CTL and TAM; 3) genes with over 0.95 quantile of pagerank centrality. The *Right* shows GO enrichment of genes with the most affected pagerank centrality. The genes listed in the network analysis (*Left*) are in orange-red (CTL) and blue (TAM) colors in the GO enrichment analysis. (B) The dot plot shows prenatal TAM administration reduced the number of cells expressing *Wnt8b*, *Dmrt2*, *Hes1*, *Lrp6*, *Acvr2b*, and *Sox3*. (C) TAM treatment expanded *Wnt8b* expression laterally in the cortex ( $P < 0.0001$ , two-way ANOVA, box1,  $P = 0.0047$ ; box2,  $P = 0.0012$ ; box3,  $P = 0.2137$ ; box4-6,  $P > 0.9999$ ; box7,  $P = 0.4281$ ; box8,  $P = 0.0008$ ; box9,  $P = 0.0003$ . CTL  $n = 9$ , TAM  $n = 9$ ). The cortex above the CH was separated by continuous bins and ISH staining puncta were quantified in each bin. The enlarged images on the *Right* show bin-7 and -8. N.S., nonsignificant. (Scale bar, 100  $\mu\text{m}$ .) ISH assays show reduced expression of *Lrp6*, *Dmrt2*, *Hes1*, and *Sox3* mRNAs in TAM-treated brains (*Lrp6*,  $P = 0.0023$ , CTL  $n = 12$ , TAM  $n = 18$ ; *Dmrt2*,  $P < 0.0001$ , CTL  $n = 15$ , TAM  $n = 15$ ; *Hes1*,  $P < 0.0001$ , CTL  $n = 15$ , TAM  $n = 17$ ; *Sox3*,  $P < 0.0001$ , CTL  $n = 12$ , TAM  $n = 12$ ). (Scale bar, 200  $\mu\text{m}$ .) \*,  $0.01 \leq P < 0.05$ ; \*\*,  $P < 0.01$ .



CTL =  $1.7 \pm 0.58$ , TAM =  $3.0 \pm 0.96$ ; bin9, CTL =  $0.58 \pm 0.10$ , TAM =  $2.0 \pm 0.37$  and *Lpp6*: CTL =  $8.5 \pm 1.1$ , TAM =  $7.0 \pm 1.1$  and *Dmrta2*: CTL =  $8.7 \pm 1.7$ , TAM =  $5.7 \pm 0.9$  and *Hes1*: CTL =  $9.4 \pm 0.7$ , TAM =  $6.0 \pm 0.9$  and *Avc2b*: CTL =  $9.8 \pm 1.4$ , TAM =  $6.4 \pm 1.6$ ; mean  $\pm$  SD) (Fig. 4C and *SI Appendix*, Fig. S5A). We also verified the reduced expression of a neural progenitor marker, *Sox3*, in TAM-treated brains (CTL =  $7.6 \pm 1.6$  puncta/cell, TAM =  $5.2 \pm 1.2$  puncta/cell; mean  $\pm$  SD) (Fig. 4C) (30).

Along with neural progenitor fate maintenance, *Dmrta2* has been shown to be involved in cortical patterning (31, 32). By using a conventional *Dmrta2* null mouse line, Saulnier et al. showed that in the major telencephalic patterning centers, the roof plate, and cortical hem, loss of *Dmrta2* resulted in decreased expression of Wnt and BMP signaling genes, such as *Wnt8b* (31). Our scRNA-seq analysis showed that TAM treatment dysregulated the expression of Wnts, Bmps, and their receptors and cytoplasmic modulators in NPCs and cells in the cortical hem (Fig. 4A–C and *SI Appendix*, Fig. S4). We found TAM treatment expanded *Wnt8b* expression from ventral-medial to dorsal-lateral regions (Fig. 4C). Therefore, dysregulation of Wnt and BMP pathways may be one of the underlying mechanisms that control cortical patterning changes in TAM-treated brains.

In summary, our data revealed that TAM administration altered the landscape of gene regulatory network in NPCs and CH cells by reducing intramodular connectivity and gene expression heterogeneity. Particularly, TAM administration at the early stage of cortical neurogenesis dramatically attenuated the Wnt signaling network. In addition to Wnt and *Dmrta2* regulations, the scRNA-seq analysis showed TAM also perturbed the expression of genes that have been shown to be involved in other signaling pathways, such as *Fgf* (e.g., *Ptpn11*), Notch (e.g., *Hes5*, *Snn1*, *Ctbp1*, *Ctbp2*, *Hdac1*, and *Hdac2*), and sonic hedgehog (*Shh*) (e.g., *Prkar1a* and *Smo*) (*SI Appendix*, Fig. S4).

**TAM Directly Regulated Neural Proliferation and Differentiation via Wnt-Dmrta2 Signaling.** To demonstrate the causal effect of Wnt and BMP pathways on NPC proliferation and differentiation, we carried out rescue assays using two Wnt agonists (Wnt agonist 1 and HLY78) and a BMP agonist (SJ000291942). Wnt agonist 1 is a pan-Wnt signaling pathway activator, which induces Ctnnb1 ( $\beta$ -catenin)- and Tcf-dependent transcriptional activity (33). HLY78 potentiates the Axin-Lrp6 association, and thus promotes Lrp6 phosphorylation and Wnt signaling transduction (34). SJ000291942 activates the canonical BMP signaling pathway (35).

Single cells were dissociated from E11 mouse cortex and cultured with a TAM active metabolite, 4-hydroxy-tamoxifen (4-OH-TAM) and one of the agonists in vitro for 16 h. Neuron and NPC pair cells were detected by *Tubb3* and *Nes* immunostaining (neuron pair cells, N/N; NPC pair cell, P/P) (Fig. 5A, *Upper Right* diagram). The pair-cell assay showed that 4-OH-TAM produced more neuron pair cells (N/N ratio: CTL =  $0.48 \pm 0.08$ , 4-OH-TAM =  $0.73 \pm 0.3$ ; mean  $\pm$  SD) than the control and reduced the numbers of progenitor pairs (P/P ratio: CTL =  $0.49 \pm 0.08$ , 4-OH-TAM =  $0.16 \pm 0.2\%$ ; mean  $\pm$  SD) (Fig. 5A). Adding Wnt agonists rescued the TAM effects on progenitor cell proliferation and differentiation (P/P ratio: CTL =  $0.49 \pm 0.08$ , 4-OH-TAM and Wnt agonist 1 =  $0.44 \pm 0.23$ , 4-OH-TAM and HLY78 =  $0.54 \pm 0.1$ . N/N ratio: CTL =  $0.48 \pm 0.08$ , 4-OH-TAM and Wnt agonist 1 =  $0.37 \pm 0.18$ , 4-OH-TAM and HLY78 =  $0.43 \pm 0.11$ ; mean  $\pm$  SD) (Fig. 5A and *SI Appendix*, Fig. S5B). We observed less rescue effects when using the BMP agonist, SJ000291942 in 4-OH-TAM-treated NPCs (P/P ratio: 4-OH-TAM and SJ000291942 =  $0.73 \pm 0.2$ ; N/N ratio: 4-OH-TAM and SJ000291942 =  $0.27 \pm 0.19$ ; mean  $\pm$  SD) (*SI Appendix*, Fig. S5B). The numbers of asymmetrically dividing cells (P/N) were not significantly altered in all conditions. Expectedly, the total number of *Mki67*<sup>+</sup> cells in 4-OH-TAM-treated E11 NPCs was also reduced (*SI Appendix*, Fig. S5C).

To further demonstrate the function of the critical gene, *Dmrta2* in regulating cell differentiation, we infected E11 NPCs with *Dmrta2* overexpression (*Dmrta2*OE) and negative GFP control lentiviral particles. The expression of *Dmrta2* and GFP (*Dmrta2*-IRES2-GFP) was driven by the EF-1 $\alpha$  promoter. After 4 d, we replated *Dmrta2* overexpressing and control NPCs in a single-cell density and added 4-OH-TAM. After 16 h, we performed immunostaining and quantified the numbers of NPC and neuronal pair cells (Fig. 5B, the *Left* diagram). We found overexpression of *Dmrta2* in E11 cortex-derived NPCs counteracted the effects of TAM on NPC fate specification (P/P ratio: CTL =  $0.53 \pm 0.05$ , *Dmrta2*OE =  $0.65 \pm 0.08$ , 4-OH-TAM =  $0.39 \pm 0.05$ , *Dmrta2*OE and 4-OH-TAM =  $0.50 \pm 0.06\%$ . N/N ratio: CTL =  $0.38 \pm 0.06$ , *Dmrta2*OE =  $0.24 \pm 0.07$ , 4-OH-TAM =  $0.52 \pm 0.06$ , *Dmrta2*OE and 4-OH-TAM =  $0.42 \pm 0.08$ ; mean  $\pm$  SD) (Fig. 5B).

As a proof of principle, we showed a tight link between TAM and Wnt8b-*Dmrta2* regulatory axis in regulating NPC fate specification. TAM treatment dysregulates this pathway and results in deficits in cortical neurogenesis and patterning in prenatal and postnatal offspring.

**TAM Inhibited Adult Neural Progenitor Cell Proliferation in Both the SVZ and the DG.** In adult mice, several studies reported acute but not long-lasting effects of TAM treatment on locomotion, exploration, anxiety behaviors, and learning and memory in mice (36–39). To study the potential influence of TAM on adult neurogenesis, we employed an established 5-d protocol that was used for CreER/LoxP-dependent gene targeting in adult mice (40). We injected 2 mg TAM/day to 3- to 4-wk-old male C57BL/6 mice continuously for 5 d. One dose of BrdU was administered on the second day of TAM injection. The brains were analyzed 5 d after the last TAM administration. We found that TAM greatly reduced the number of BrdU- and *Mki67*-labeled proliferating cells in the SVZ (BrdU: CTL =  $12.1 \pm 3.8\%$ , TAM =  $7.2 \pm 2.3\%$  and *Mki67*: CTL =  $17.7 \pm 3.6\%$ , TAM =  $11.7 \pm 4.6\%$ ; mean  $\pm$  SD) and in the DG (BrdU: CTL =  $16.1 \pm 4.7$ , TAM =  $7.1 \pm 2$  and *Mki67*: CTL =  $13.2 \pm 5.2$ , TAM =  $7.2 \pm 3.4$ ; mean  $\pm$  SD) (Fig. 6A). To test the effect of TAM dosage, we reduced the TAM dose to 1 mg/animal per day and the frequency of TAM treatment to two injections. The mice received two BrdU injections 12 h and 24 h after the first TAM administration. The brain samples were analyzed 96 h after the initial TAM injection. We observed the same effect of reduced proliferating cells in the SVZ of the caudate putamen as in the high TAM dosage group (BrdU: CTL =  $27.3 \pm 9.4\%$ , TAM =  $15.4 \pm 6.1\%$  and *Mki67*: CTL =  $26.4 \pm 3.7\%$ , TAM =  $21.6 \pm 3.0\%$ ; mean  $\pm$  SD) (Fig. 6B). There was no detectable cell apoptosis after 5 d of TAM treatment (2 mg/animal/day) (*SI Appendix*, Fig. S6A) and administration of TAM did not significantly change overall dendritic complexity in adult brains (*SI Appendix*, Fig. S6B).

## Discussions

In the current study, we showed that a single-dose, prenatal TAM exposure dramatically changes the global gene expression landscapes of cells in the cerebral hemisphere and has long-lasting influence on cortical neurogenesis, patterning, and neural circuit formation in perinatal and postnatal offspring.

Normal cortical development requires a period of extensive NPC proliferation accompanied by differentiation. Ensuring precise coordination between cell division, cell cycle exit, and differentiation is essential to generate diverse functional neurons and glial cells (41). It has been demonstrated that the G1 phase is critical in determining the cell fates and nearly all G1 regulators impact neurogenesis (42). Young et al. showed that loss of *Dmrta2* increased the number of cells in the G1/G0 phase after a 6-d differentiation of mouse NPCs, decreased the number of cells in the S phase, and increased the number of cells expressing

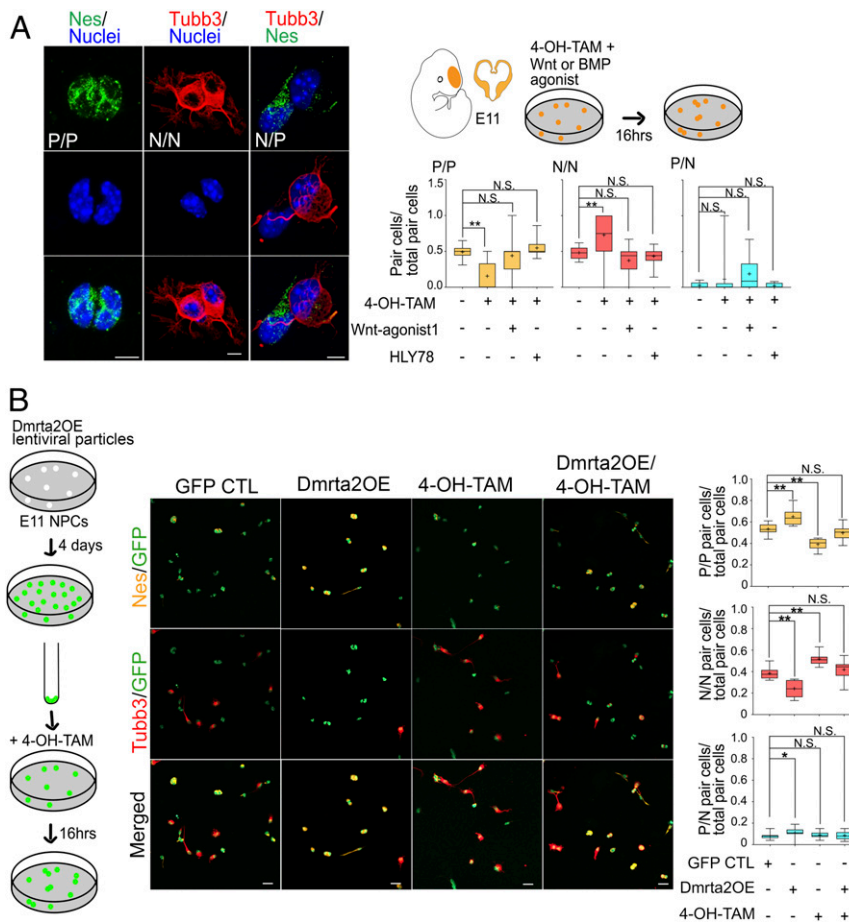


**Fig. 5.** TAM directly affects the Wnt-Dmrt2 signaling pathway in regulating NPC fate specification. (A) Pair cell assay showed that treatment of E11 cortical NPCs with Wnt agonists, Wnt agonist 1 and HLY78, rescued the effects of 4-OH-TAM on E11 NPC fate specification (P/P: CTL vs. 4-OH-TAM,  $P < 0.0001$ ; CTL vs. 4-OH-TAM and Wnt agonist 1,  $P = 0.3821$ ; CTL vs. 4-OH-TAM and HLY78,  $P = 0.2123$ ; CTL vs. 4-OH-TAM and SJ00291942,  $P = 0.0031$ . N/N: CTL vs. 4-OH-TAM,  $P < 0.0001$ ; CTL vs. 4-OH-TAM and Wnt agonist 1,  $P = 0.1154$ ; CTL vs. 4-OH-TAM and HLY78,  $P = 0.3084$ ; CTL vs. 4-OH-TAM and SJ00291942,  $P = 0.0015$ . N/P: CTL vs. 4-OH-TAM,  $P = 0.8399$ ; CTL vs. 4-OH-TAM and Wnt agonist 1,  $P = 0.1000$ ; CTL vs. 4-OH-TAM and HLY78,  $P = 0.6063$ ; CTL vs. 4-OH-TAM and SJ00291942,  $P = 0.6728$ . Mann-Whitney  $U$  test, CTL  $n = 34$ , 4-OH-TAM  $n = 33$ ). (Scale bar, 5  $\mu\text{m}$ .) N, neuron; P, progenitor. Tubb3, neuron-specific class III  $\beta$ -tubulin; Nes, nestin. (B) Overexpression of *Dmrt2* in 4-OH-TAM-treated NPCs rescued cell proliferation and differentiation (P/P: GFP CTL vs. Dmrt2OE/4-OH-TAM,  $P = 0.1463$ ; N/N: GFP CTL vs. Dmrt2OE,  $P < 0.0001$ ; GFP CTL vs. Dmrt2OE and 4-OH-TAM,  $P = 0.1467$ . P/N: GFP CTL vs. Dmrt2OE,  $P = 0.0421$ ; GFP CTL vs. 4-OH-TAM,  $P = 0.8749$ ; GFP CTL vs. Dmrt2OE and 4-OH-TAM,  $P = 0.4412$ . GFP CTL,  $n = 12$ ; 4-OH-TAM,  $n = 12$ , Mann-Whitney  $U$  test). (Scale bar, 20  $\mu\text{m}$ .) \*,  $0.01 \leq P < 0.05$ ; \*\* $P < 0.01$ . N.S., nonsignificant.

*Cdkn1b* and *Cdkn1c* (17). Moreover, Davidson et al. showed that the phosphorylation of Lrp6 is regulated by a cyclin-dependent kinase L63 and cyclin Y at G2/M phase in *Drosophila* and *Xenopus* (43). In Pax6<sup>+</sup> cortical NPCs, TAM treatment down-regulated the expression of cyclin and Cdk genes that promote G1/S and G2/M progression. TAM treatment increased the expression of G1 phase arrest genes, such as *Cdkn1c* and *Cdkn2d*, in newborn cortical neurons (SI Appendix, Fig. S7). Moreover, TAM also represses the expression of *Gsk3b* and *Axin2*, which together with *Ctnnb1* have been shown to accumulate at the centrosome to ensure a proper distribution of the chromosomes during M phase (SI Appendix, Fig. S4) (44–46). These data suggest that TAM could suppress cell cycle progression by targeting cyclin/Cdk genes and genes in Wnt signaling in early-stage NPCs, such as neuroepithelial cells and radial glial cells, while it promotes expression of G1 phase inhibitors in later-stage NPCs, probably intermediate progenitors, and thus leads to prolonged G1 phase and subsequent advanced neuronal gene expression and precocious neuronal differentiation.

It is well known that there are critical periods for the establishment of certain types of neural plasticity and at those times

individuals are most vulnerable to external disturbances. Our previous study showed perturbation of this critical time in prenatal brains has life-long effects on cortical neural network formation and learning and memory behaviors in adults (47). In the current study, we showed that a single low-dose TAM administration at the early stage of cortical neurogenesis (E8 to E10) impairs cortical neurogenesis, dendritic morphogenesis, synaptic formation, gliogenesis, and possible axon formation in postnatal offspring (Fig. 3 F–H and SI Appendix, Figs. S2B and 3A). Although the evidence that loss of *Dmrt2* impairs commissural axonal tracts and thalamocortical axon formation may explain the axon formation defects in TAM-treated brain (31), the mechanisms of how TAM regulates dendritic and synaptic formation are still elusive. Our scRNA-seq analysis of E12 embryonic brains may not reveal a comprehensive picture of TAM's effects on neurogenesis and neural circuit formation in postnatal offspring. Therefore, detailed, developmental stage-specific scRNA-seq analyses would be needed to further dissect the underlying mechanisms of the long-lasting effects of TAM.

Estrogens have been shown to promote NPC proliferation and differentiation, neurite elongation, and synaptic formation during

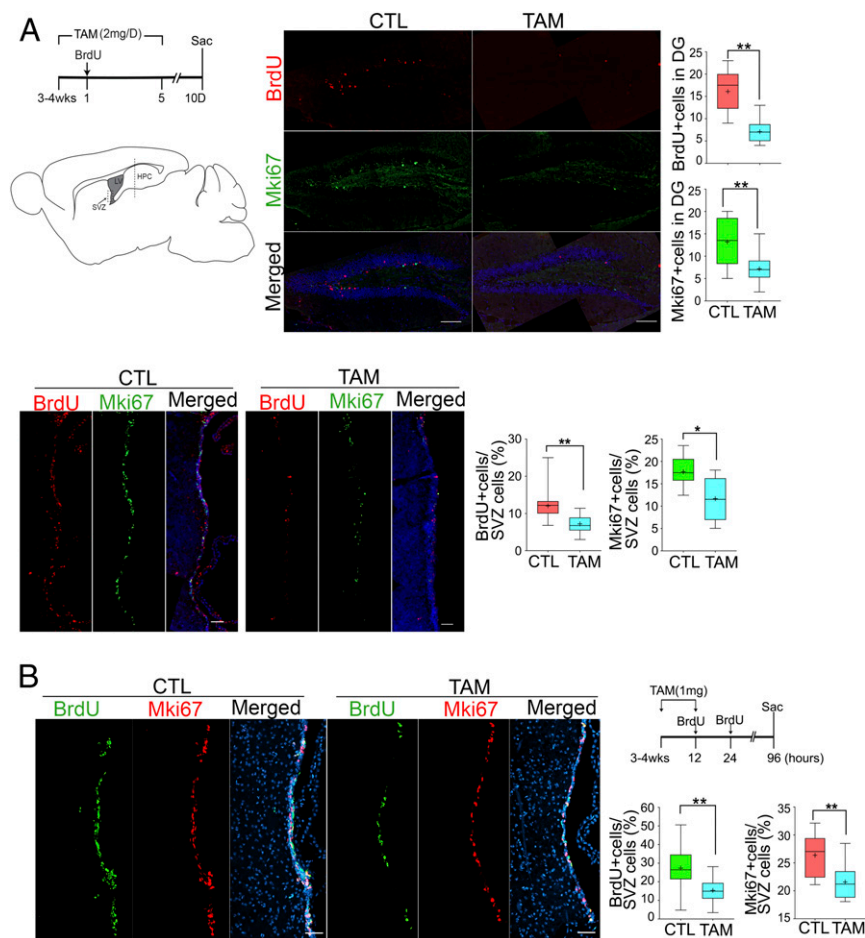


**Fig. 6.** TAM inhibits adult neural stem cell proliferation in both the SVZ of the forebrain and the DG of the hippocampus. (A) The 3- to 4-wk-old mice were injected with 2 mg TAM per day for 5 consecutive days. BrdU was administered on the second day of TAM injection. Samples were collected 10 d after the initial TAM administration (Upper Left). TAM treatment dramatically decreased number of cells expressing either BrdU or Mki67 in the SVZ (BrdU,  $P < 0.0001$ , Mann-Whitney  $U$  test, CTL  $n = 23$ , TAM  $n = 24$ ; Mki67,  $P = 0.0181$ , Mann-Whitney  $U$  test, CTL  $n = 15$ , TAM  $n = 15$ ) and in the DG (BrdU,  $P < 0.0001$ , Mann-Whitney  $U$  test, CTL  $n = 12$ , TAM  $n = 12$ ; Mki67,  $P = 0.0028$ , Mann-Whitney  $U$  test, CTL  $n = 12$ , TAM  $n = 12$ ). (Scale bar, 50  $\mu\text{m}$ .) LV, lateral ventricle; HPC, hippocampus. (B) The 3- to 4-wk-old mice were injected with two doses of TAM (1 mg/mouse) at 12 h and 24 h after the first TAM injection. Samples were collected 96 h after the initial TAM administration. TAM treatment decreased the numbers of BrdU<sup>+</sup> and Mki67<sup>+</sup> cells in the SVZ (BrdU,  $P = 0.0187$ , Mann-Whitney  $U$  test, CTL  $n = 36$ , TAM  $n = 31$ ; Mki67,  $P = 0.0021$ , Mann-Whitney  $U$  test, CTL  $n = 36$ , TAM  $n = 31$ ). (Scale bar, 50  $\mu\text{m}$ .) \*,  $0.01 \leq P < 0.05$ ; \*\* $P < 0.01$ .

the later stage of corticogenesis (48–50). It seems that TAM and estrogen treatments showed somewhat opposite phenomena in terms of NPC proliferation and differentiation, suggesting TAM may function through interfering with the estrogen signaling pathway. Our scRNA-seq analysis showed that expression of major estrogen receptors, estrogen receptor 1 (*Esr1*), *Esr2*, estrogen-related receptor beta (*Esrβ*), and a critical estrogen synthetic enzyme, aromatase (*Cyp19a1*) were undetectable. The expression levels of two other estrogen receptors, estrogen-related receptor alpha (*Esrα*) and G Protein-Coupled Estrogen Receptor 1 (*Gper1*) were extremely low at E12 in the telencephalon (SI Appendix, Fig. S8A), indicating that TAM may function via an estrogen receptor-independent mechanism in regulating cell fates and neural networks. To this end, we examined the expression of the estrogen receptor-independent, TAM-regulated genes in our E12 scRNA-seq data (51, 52). TAM treatment slightly perturbed the expression of estrogen receptor-independent genes that regulate cell cycle progression (e.g., *Cdk2*, *Cdk7*, *Cdk9*, and *Ccnd1*), neurogenesis, and dendrite and axon formations (SI Appendix, Fig. S8B). For example, TAM treatment reduced the expression of critical components of the Fgf signaling pathway (e.g., *Fgf1*) and Akt-mTOR pathway (e.g., *Akt1* and *Mtor*)

at expression level and cell percentages which may block NPC proliferation (53–57) and impair cell fate specification (56, 58–62). Moreover, a great deal of evidence has shown that perturbation of mTOR and Fgf pathways greatly impairs neural circuit assembly, including axon formation (63–65), dendritic morphogenesis (66, 67), and synaptic formation (68, 69). Considered together, it appears that TAM treatment might influence corticogenesis via an estrogen receptor-independent manner at early-middle stages of neurogenesis.

The TAM-inducible CreER/LoxP system laid the foundations of significant discoveries in adult and embryonic neural stem cell fate mapping (2, 10, 11, 70), gene functions (71), as well as neuronal subtypes and activity-dependent neural circuitry (72–74). It seems that the side effect of TAM could be a vulnerable Achilles' heel for TAM-induced CreER/LoxP cell lineage tracing and/or genetic targeting studies. Therefore, special care should be taken when using the CreER/LoxP system for neural lineage tracing study, because its results are not falsifiable due to lack of appropriate controls.

## Materials and Methods

**Experimental Animals.** Mice were kept and fed in standard conditions on a 12-h light/dark cycle. Experimental procedures on animals were performed in



accordance with the guidelines of University of California, Los Angeles (UCLA) Institutional Animal Care and Use Committee and UCLA Animal Research Committee. Three different genetic background lines were used: C57BL/6J, Crl:CD1(ICR), and the Prom1-creER/ZsGreen transgenic line, which was generated by crossing the Prom1<sup>tm1(cre/ERT2)Glib</sup> line (129S6/SvEvTac background) and the Gt(ROSA)26Sor<sup>tm6(CAG-ZsGreen1)Hze</sup> (129S6/SvEvTac × C57BL/6Ncrl background, JAX). Details are given in *SI Appendix*.

**TAM Administration and Fostering.** TAM (Sigma, T5648) was suspended in corn oil to a stock concentration of 20 mg/mL. Tamoxifen was administered by IP injection. To obtain postnatal offspring, a caesarean section was performed on pregnant dams in the afternoon on E18 and pups were fostered to CD1 or 129S6 dams. Details are given in *SI Appendix*.

**Single-Cell RNA-Seq Analysis.** The forebrains were collected at E12, dissociated in papain (BrainBits, LLC). To minimize potential variability between individuals, samples were pooled from three litters per experimental condition. The cell viability was assessed by Trypan blue staining. The cells were diluted to a final concentration of  $1 \times 10^6$ /mL and 10,000 single-cell gel beads in emulsion per sample was loaded onto the Chromium Controller (10× Genomics). The raw reads were converted to molecule counts using the Cell Ranger pipeline, followed by the process using the Seurat R toolkit. The cell numbers of CTL and TAM datasets were then normalized by random section of 4,193 cells/condition. Based on UMAP plot, 14 clusters were classified using the function *FindClusters*. To identify the marker genes of each cluster, function *FindAllMarkers* with likelihood-ratio test was applied. The NPC1, NPC2, and CH clusters of each condition (CTL and TAM) were merged and served as the input for inferring the putative gene-to-gene correlated network using the bigScale2 algorithm (28). The network centrality pagerank was chosen to represent the gene essentiality. Details are given in *SI Appendix*.

**EdU/BrdU Double Labeling Assay.** Details are given in *SI Appendix*.

**BrdU Administration.** Details are given in *SI Appendix*.

1. D. Metzger, J. Clifford, H. Chiba, P. Chambon, Conditional site-specific recombination in mammalian cells using a ligand-dependent chimeric Cre recombinase. *Proc. Natl. Acad. Sci. U.S.A.* **92**, 6991–6995 (1995).
2. A. M. Bond, G. L. Ming, H. Song, Adult mammalian neural stem cells and neurogenesis: Five decades later. *Cell Stem Cell* **17**, 385–395 (2015).
3. K. Kretschmar, F. M. Watt, Lineage tracing. *Cell* **148**, 33–45 (2012).
4. A. Visel *et al.*, A high-resolution enhancer atlas of the developing telencephalon. *Cell* **152**, 895–908 (2013).
5. J. Cuzick *et al.*; IBIS-I Investigators, Tamoxifen for prevention of breast cancer: Extended long-term follow-up of the IBIS-I breast cancer prevention trial. *Lancet Oncol.* **16**, 67–75 (2015).
6. G. Braems, H. Denys, O. De Wever, V. Cocquyt, R. Van den Broecke, Use of tamoxifen before and during pregnancy. *Oncologist* **16**, 1547–1551 (2011).
7. L. Barthelmes, C. A. Gateley, Tamoxifen and pregnancy. *Breast* **13**, 446–451 (2004).
8. E. Koca *et al.*, Safety of tamoxifen during pregnancy: 3 case reports and review of the literature. *Breast Care (Base)* **8**, 453–454 (2013).
9. B. Jyoti, C. Bharat, N. Ankita, B. Munita, G. Sudeep, Pregnancy on tamoxifen: Case-report and review of literature. *South Asian J. Cancer* **5**, 209–210 (2016).
10. P. Gao *et al.*, Deterministic progenitor behavior and unitary production of neurons in the neocortex. *Cell* **159**, 775–788 (2014).
11. D. A. Berg *et al.*, A common embryonic origin of stem cells drives developmental and adult neurogenesis. *Cell* **177**, 654–668.e15 (2019).
12. P. A. Georgala, M. Manuel, D. J. Price, The generation of superficial cortical layers is regulated by levels of the transcription factor Pax6. *Cereb. Cortex* **21**, 81–94 (2011).
13. I. Imayoshi, M. Sakamoto, M. Yamaguchi, K. Mori, R. Kageyama, Essential roles of Notch signaling in maintenance of neural stem cells in developing and adult brains. *J. Neurosci.* **30**, 3489–3498 (2010).
14. B. Lizen, M. Claus, L. Jeannotte, F. M. Rijli, F. Gofflot, Perinatal induction of Cre recombination with tamoxifen. *Transgenic Res.* **24**, 1065–1077 (2015).
15. P. S. Danielian, D. Muccino, D. H. Rowitch, S. K. Michael, A. P. McMahon, Modification of gene activity in mouse embryos in utero by a tamoxifen-inducible form of Cre recombinase. *Curr. Biol.* **8**, 1323–1326 (1998).
16. S.-S. Yuki Nakamura, Takaki Miyata, Masaharu Ogawa, Takuya Shimazaki, Samuel Weiss, Ryoichiro Kageyama, and Hideyuki Okano, the bHLH gene Hes1 as a repressor of the neuronal commitment of CNS stem cells. *J. Neurosci.* **20**, 283–293 (2000).
17. F. I. Young *et al.*, The doublesex-related Dmrt2 safeguards neural progenitor maintenance involving transcriptional regulation of Hes1. *Proc. Natl. Acad. Sci. U.S.A.* **114**, E5599–E5607 (2017).
18. S. Hayashi, A. P. McMahon, Efficient recombination in diverse tissues by a tamoxifen-inducible form of Cre: A tool for temporally regulated gene activation/inactivation in the mouse. *Dev. Biol.* **244**, 305–318 (2002).
19. B. J. Molyneaux, P. Arlotta, J. R. Menezes, J. D. Macklis, Neuronal subtype specification in the cerebral cortex. *Nat. Rev. Neurosci.* **8**, 427–437 (2007).

**In Vitro Rescue Assay.** E11 C57BL/6 mouse forebrains were collected and dissociated to single cells. The cells were treated with 4-OH-TAM (Sigma, H6278) and Wnt agonist 1, HLY78, or a BMP agonist SJ000291942. For Dmrt2 rescue assay, E11 NPCs were infected with Dmrt2 overexpression and control lentiviral particles and then treated with 4-OH-TAM. The cells were fixed with 4% paraformaldehyde after 16 h. Details are given in *SI Appendix*.

**ISH.** Fluorescent ISH assay was performed following manufacturer's instructions (Advanced Cell Diagnostics, Inc.). Details are given in *SI Appendix*.

**Immunohistochemistry.** Details are given in *SI Appendix*.

**Golgi-Cox Staining and TUNEL Assay.** Details are given in *SI Appendix*.

**Synaptic Puncta Imaging and Image Processes.** The synaptic puncta were acquired using a 63× oil immersion objective lens, NA = 1.4 (Planapo; Zeiss). A z-step of 0.2-μm intervals was used. The pre- and postsynaptic puncta were analyzed as described in our previous study (47).

**Imaging Quantification and Statistical Analysis.** Images obtained were processed and quantified with Imaris software. Mann-Whitney U test, one-way ANOVA, and two-way ANOVA were used to assess statistical significance between independent experimental groups. Details are given in *SI Appendix*.

**Data Availability.** The sequences reported in this paper have been deposited in Gene Expression Omnibus (GEO) database, <https://www.ncbi.nlm.nih.gov/geo/> (accession no. GSE152125).

**ACKNOWLEDGMENTS.** We thank the Intellectual and Developmental Disabilities Research Center at the University of California, Los Angeles, supported by NIH Grant U54HD087101 and National Key Research and Development Program (2016YFA0100801). This work was supported by NIH/National Institute of Mental Health Grant 5R21MH115382 (Q.L. and Y.E.S.).

20. R. Satija, J. A. Farrell, D. Gennert, A. F. Schier, A. Regev, Spatial reconstruction of single-cell gene expression data. *Nat. Biotechnol.* **33**, 495–502 (2015).
21. A. Butler, P. Hoffman, P. Smibert, E. Papalexi, R. Satija, Integrating single-cell transcriptomic data across different conditions, technologies, and species. *Nat. Biotechnol.* **36**, 411–420 (2018).
22. D. D. O'Leary, S. J. Chou, S. Sahara, Area patterning of the mammalian cortex. *Neuron* **56**, 252–269 (2007).
23. A. S. E. Cuomo *et al.*; HipSci Consortium, Single-cell RNA-sequencing of differentiating iPSCs reveals dynamic genetic effects on gene expression. *Nat. Commun.* **11**, 810 (2020).
24. C. Mayer *et al.*, Developmental diversification of cortical inhibitory interneurons. *Nature* **555**, 457–462 (2018).
25. B. Martynoga, H. Morrison, D. J. Price, J. O. Mason, Foxg1 is required for specification of ventral telencephalon and region-specific regulation of dorsal telencephalic precursor proliferation and apoptosis. *Dev. Biol.* **283**, 113–127 (2005).
26. M. J. Hendzel *et al.*, Mitosis-specific phosphorylation of histone H3 initiates primarily within pericentromeric heterochromatin during G2 and spreads in an ordered fashion coincident with mitotic chromosome condensation. *Chromosoma* **106**, 348–360 (1997).
27. M. Marin-Padilla, Cajal-Retzius cells and the development of the neocortex. *Trends Neurosci.* **21**, 64–71 (1998).
28. G. Iacono, R. Massoni-Badosa, H. Heyn, Single-cell transcriptomics unveils gene regulatory network plasticity. *Genome Biol.* **20**, 110 (2019).
29. A. Kriegstein, S. Noctor, V. Martinez-Cerdeño, Patterns of neural stem and progenitor cell division may underlie evolutionary cortical expansion. *Nat. Rev. Neurosci.* **7**, 883–890 (2006).
30. N. Rogers *et al.*, Expression of the murine transcription factor SOX3 during embryonic and adult neurogenesis. *Gene Expr. Patterns* **13**, 240–248 (2013).
31. A. Saulnier *et al.*, The doublesex homolog Dmrt5 is required for the development of the caudomedial cerebral cortex in mammals. *Cereb. Cortex* **23**, 2552–2567 (2013).
32. S. De Clercq *et al.*, DMRT5 together with DMRT3 directly controls Hippocampus development and neocortical area Map formation. *Cereb. Cortex* **28**, 493–509 (2018).
33. J. Liu *et al.*, A small-molecule agonist of the Wnt signaling pathway. *Angew. Chem. Int. Ed. Engl.* **44**, 1987–1990 (2005).
34. S. Wang *et al.*, Small-molecule modulation of Wnt signaling via modulating the Axin-LRP5/6 interaction. *Nat. Chem. Biol.* **9**, 579–585 (2013).
35. J. R. Genthé *et al.*, Ventromorphins: A new class of small molecule activators of the canonical BMP signaling pathway. *ACS Chem. Biol.* **12**, 2436–2447 (2017).
36. D. Chen, C. F. Wu, B. Shi, Y. M. Xu, Tamoxifen and toremifene impair retrieval, but not acquisition, of spatial information processing in mice. *Pharmacol. Biochem. Behav.* **72**, 417–421 (2002).

37. D. Chen, C. F. Wu, B. Shi, Y. M. Xu, Tamoxifen and toremifene cause impairment of learning and memory function in mice. *Pharmacol. Biochem. Behav.* **71**, 269–276 (2002).
38. M. A. Vogt *et al.*, Suitability of tamoxifen-induced mutagenesis for behavioral phenotyping. *Exp. Neurol.* **211**, 25–33 (2008).
39. P. Rotheneichner *et al.*, Tamoxifen activation of cre-recombinase has No persisting effects on adult neurogenesis or learning and anxiety. *Front. Neurosci.* **11**, 27 (2017).
40. G. Erdmann, G. Schütz, S. Berger, Inducible gene inactivation in neurons of the adult mouse forebrain. *BMC Neurosci.* **8**, 63 (2007).
41. C. Dehay, H. Kennedy, Cell-cycle control and cortical development. *Nat. Rev. Neurosci.* **8**, 438–450 (2007).
42. C. Hindley, A. Philpott, Co-ordination of cell cycle and differentiation in the developing nervous system. *Biochem. J.* **444**, 375–382 (2012).
43. G. Davidson *et al.*, Cell cycle control of wnt receptor activation. *Dev. Cell* **17**, 788–799 (2009).
44. P. Huang, T. Senga, M. Hamaguchi, A novel role of phospho-beta-catenin in microtubule regrowth at centrosome. *Oncogene* **26**, 4357–4371 (2007).
45. S. Bahmanyar *et al.*, beta-Catenin is a Nek2 substrate involved in centrosome separation. *Genes Dev.* **22**, 91–105 (2008).
46. M. V. Hadjihannas *et al.*, Aberrant Wnt/beta-catenin signaling can induce chromosomal instability in colon cancer. *Proc. Natl. Acad. Sci. U.S.A.* **103**, 10747–10752 (2006).
47. Q. Lin *et al.*, MicroRNA-mediated disruption of dendritogenesis during a critical period of development influences cognitive capacity later in life. *Proc. Natl. Acad. Sci. U.S.A.* **114**, 9188–9193 (2017).
48. C. Beyer, Estrogen and the developing mammalian brain. *Anat. Embryol. (Berl.)* **199**, 379–390 (1999).
49. M. C. S. Denley, N. J. F. Gatford, K. J. Sellers, D. P. Srivastava, Estradiol and the development of the cerebral cortex: An unexpected role? *Front. Neurosci.* **12**, 245 (2018).
50. B. S. McEwen, S. E. Alves, Estrogen actions in the central nervous system. *Endocr. Rev.* **20**, 279–307 (1999).
51. T. A. Bogush *et al.*, Tamoxifen never ceases to amaze: New findings on non-estrogen receptor molecular targets and mediated effects. *Cancer Invest.* **36**, 211–220 (2018).
52. T. Bogush *et al.*, Tamoxifen non-estrogen receptor mediated molecular targets. *Oncol. Rev.* **6**, e15 (2012).
53. A. D. Sinor, L. Lillien, Akt-1 expression level regulates CNS precursors. *J. Neurosci.* **24**, 8531–8541 (2004).
54. B. P. Zhou *et al.*, Cytoplasmic localization of p21Cip1/WAF1 by Akt-induced phosphorylation in HER-2/neu-overexpressing cells. *Nat. Cell Biol.* **3**, 245–252 (2001).
55. H. Paek, G. Gutin, J. M. Hébert, FGF signaling is strictly required to maintain early telencephalic precursor cell survival. *Development* **136**, 2457–2465 (2009).
56. M. Ka, G. Condorelli, J. R. Woodgett, W. Y. Kim, mTOR regulates brain morphogenesis by mediating GSK3 signaling. *Development* **141**, 4076–4086 (2014).
57. S. D. Wahane *et al.*, PI3K-p110-alpha-subtype signalling mediates survival, proliferation and neurogenesis of cortical progenitor cells via activation of mTORC2. *J. Neurochem.* **130**, 255–267 (2014).
58. N. W. Hartman *et al.*, mTORC1 targets the translational repressor 4E-BP2, but not S6 kinase 1/2, to regulate neural stem cell self-renewal in vivo. *Cell Rep.* **5**, 433–444 (2013).
59. L. Magri *et al.*, Timing of mTOR activation affects tuberous sclerosis complex neuropathology in mouse models. *Dis. Model. Mech.* **6**, 1185–1197 (2013).
60. S. Sahara, D. D. O'Leary, Fgf10 regulates transition period of cortical stem cell differentiation to radial glia controlling generation of neurons and basal progenitors. *Neuron* **63**, 48–62 (2009).
61. R. Toyoda *et al.*, FGF8 acts as a classic diffusible morphogen to pattern the neocortex. *Development* **137**, 3439–3448 (2010).
62. J. M. Neugebauer, H. J. Yost, FGF signaling is required for brain left-right asymmetry and brain midline formation. *Dev. Biol.* **386**, 123–134 (2014).
63. K. J. Huffman, S. Garel, J. L. Rubenstein, Fgf8 regulates the development of intraneocortical projections. *J. Neurosci.* **24**, 8917–8923 (2004).
64. G. Szebenyi *et al.*, Fibroblast growth factor-2 promotes axon branching of cortical neurons by influencing morphology and behavior of the primary growth cone. *J. Neurosci.* **21**, 3932–3941 (2001).
65. E. M. Hur, F. Q. Zhou, GSK3 signalling in neural development. *Nat. Rev. Neurosci.* **11**, 539–551 (2010).
66. I. Nikolaeva, T. M. Kazdoba, B. Crowell, G. D'Arcangelo, Differential roles for Akt and mTORC1 in the hypertrophy of Pten mutant neurons, a cellular model of brain overgrowth disorders. *Neuroscience* **354**, 196–207 (2017).
67. J. Y. Huang, M. Lynn Miskus, H. C. Lu, FGF-FGFR mediates the activity-dependent dendritogenesis of layer IV neurons during barrel formation. *J. Neurosci.* **37**, 12094–12105 (2017).
68. A. Terauchi *et al.*, Distinct FGFs promote differentiation of excitatory and inhibitory synapses. *Nature* **465**, 783–787 (2010).
69. F. LiCausi, N. W. Hartman, Role of mTOR complexes in neurogenesis. *Int. J. Mol. Sci.* **19**, 1544 (2018).
70. L. C. Fuentealba *et al.*, Embryonic origin of postnatal neural stem cells. *Cell* **161**, 1644–1655 (2015).
71. C. T. Kuo *et al.*, Postnatal deletion of Numb/Numbl reveals repair and remodeling capacity in the subventricular neurogenic niche. *Cell* **127**, 1253–1264 (2006).
72. C. K. Kim *et al.*, Molecular and circuit-dynamical identification of top-down neural mechanisms for restraint of reward seeking. *Cell* **170**, 1013–1027.e14 (2017).
73. A. Paul *et al.*, Transcriptional architecture of synaptic communication delineates GABAergic neuron identity. *Cell* **171**, 522–539.e20 (2017).
74. L. Ye *et al.*, Wiring and molecular features of prefrontal ensembles representing distinct experiences. *Cell* **165**, 1776–1788 (2016).